Synthesis of Bamboo/Polyaniline Composites by *In Situ* Polymerization and Their Characteristics

Wen He,[a,d] Xinyu Zhang,[b] Chaoqiang Yu,[c] Dafang Huang,[a] and Yanjun Li [a,*]

Intrinsically conductive bamboo products were polymerized by the impregnation of an aniline monomer solution into a bamboo substrate and the *in situ* polymerization of PANI to obtain a semi-conducting material; the bamboo products thus obtained combined characteristics of conductivity of the PANI polymer and the strength of natural bamboo. Light microscopy and scanning electronic microscopy images showed that PANI was uniformly dispersed within the cell lumen and cell wall of the bamboo substrate. The weight percent gain and volume bulk increase of the modified bamboo were 5.18 and 14.9%, respectively. Equilibrium uptake studies showed that the modified bamboo was less hydrophilic, caused by the addition of hydrophobic PANI. The electrical conductivity of the bamboo/PANI composite ranged from 3×10^{-4} to 1×10^{-3} S cm^{-1}, which was tuned by changing the phosphate acid concentration. Fourier transform infrared spectra revealed that PANI was closely polymerized onto the cell wall, allowed by the accessibility of the amine groups of the aniline monomer to the hydroxyl groups of the bamboo matrix. Furthermore, X-ray diffraction analysis indicated that after the *in situ* polymerization of PANI, the bamboo cellulose maintained a classic cellulose structure, while its degree of crystallinity was decreased.

Keywords: Bamboo peeled veneer; Polyaniline; In situ polymerization; Electrical conductivity; X-ray diffraction

Contact information: a: College of Materials Science and Engineering, Nanjing Forestry University, Nanjing 210037, China; b: College of Light Industry Science and Engineering, Nanjing Forestry University, Nanjing 210037, China; c: College of Biology and Environment, Nanjing Forestry University, Nanjing 210037, China; d: Key Laboratory of Wood Science and Technology, Zhejiang Province;
** Corresponding author: hewen2011@njfu.edu.cn*

INTRODUCTION

Since the 1980s, electromagnetic shielding wood-based composites has started to emerge and develop as a new generation of indoor, green, and functional decorative materials for preventing electromagnetic signal leakage and external electromagnetic radiation interference. Generally, electromagnetic shielding wood-based composites are fabricated by covering the surface of a wood substrate with a conducting layer by electroless gold plating (Nagasawa 1999), metallized foils (Oka *et al.* 2004), thermal spraying (Oka *et al*. 2000), and vacuum evaporation (Oka and Hayakawa 2002). Relevant studies showed that these electromagnetic wood products exhibit good shielding effectiveness; however, to obtain stable bonding strength between wood and metal, these studies have also indicated that wood interfaces must be subjected to chemical pretreatment, which results in complex processes and higher production cost. To avoid these problems, some studies have attempted to manufacture electromagnetic wood products by heat pressing or cold pressing wood materials, in which the adhesive is mixed with inorganic conductive materials (Shuichi Kawai and Shigehisa Ishihara 1990).

Nevertheless, the results showed that the shielding effectiveness of these wood products is not stable because of the non-uniformity of inorganic materials in the adhesives (Celzard and Treusch 2005). Hence, it is important to develop some new methods for manufacturing electromagnetic wood products exhibiting a combination of good properties.

Recently, polyaniline (PANI) has attracted substantial attention as a representative conducting polymer because of its diverse molecular structure, high electrical conductivity, distinctive doping mechanism, outstanding physical properties, and good environmental stability, as well as low cost and ease of preparation (Rudge *et al*. 1994; Dalmolin *et al*. 2009; Patil *et al*. 2010). As PANI is an intrinsic conducting polymer with a conjugated electronic structure, it can be utilized as an electrical conductor after being oxidized with doping acids (Wolszczak *et al*. 1995). Furthermore, the electrical conductivity of PANI can be regulated by tuning the doping of the polymer and the protonation degree. When completely doped, PANI exhibits a conductivity of approximately 1×10^{-2} to 100 S cm^{-1}. Because of the characteristics of PANI, it is especially attractive for several applications, such as in electronic devices, batteries, solar cells, electromagnetic radiation, antistatic materials, electric heaters, and even for the filtration of heavy metals (Reza 2006; Xiang *et al*. 2011).

In practice, the difficult processability, and low solubility of PANI films in most of the available solvents limit their commercial applications, especially for their use as materials for electromagnetic shielding or in flexible optoelectronic devices (Qaiser *et al*. 2012). To solve these problems, various polymeric materials with good physical properties (*e.g.*, polystyrene, polyamides, and polysaccharides) have been combined with PANI to obtain favorable composites (Barthet *et al*. 1998; Fatyeyeva *et al*. 2011). By varying the dopant and selecting from a wide range of protonic acids, an improvement is observed with respect to the conductivity, thermal stability, processability, and adsorption (Stejskal *et al*. 1996; Trchová *et al*. 2006; Sathiyanarayanan *et al*. 2009). On the other hand, several renewable biological materials, such as wood-based cellulose, sulfonated lignin, cotton linter pulp, and saw dust, have been used as fillers to improve the mechanical properties of PANI by different processing approaches (Hu *et al*. 2011; Qaiser *et al.* 2011; Shi *et al*. 2011; 2012). These studies have shown that by using these materials, the mechanical properties and processability of PANI composites can be improved and production costs can be reduced. However, there have been no relevant studies of the impregnation of an aniline monomer solution into the wood/bamboo veneers and *in situ* polymerization of PANI to manufacture electromagnetic wood/bamboo products.

As bamboo is a vital component of forest resources, it has attracted substantial attention because of its outstanding characteristics, such as fast growth cycle, superior mechanical properties, and high yield, as well as advantages for sustainable management (Jiang 2002). Generally, as bamboo is a valuable substitute for wood, it is extensively used as raw materials for furniture, decoration, building, and transportation. Therefore, this study aims to modify bamboo peeled veneer with intrinsically conductive PANI to obtain a novel electromagnetic material. The electrical conductivity of the bamboo and PANI composite was altered by changing the concentration of the doping agent. Moreover, factors or characteristics such as weight percent gain, volume bulking, and equilibrium water uptake content of the composites were measured. In addition, the morphological characteristics and possible interface bonding of PANI within the bamboo structure as well as the X-ray diffraction (XRD) patterns of the bamboo/PANI composites were investigated. Future studies will focus on the mold and fungal durability of the modified

bamboo; also, more efforts could be focused on modifying larger dimensions of bamboo peeled veneers and investigating any gradient effects.

EXPERIMENTAL

Materials

Moso bamboo (*Phyllostachys heterocycla* cv. *pubescens*) was collected from a bamboo plantation in Anji County in Zhejiang Province, P. R. China. First, bamboo culms were subjected to rotary-cutting using a log-core veneer lathe, forming peeled veneers. Then, peeled veneers were cut into small specimens having a length and width of 20 mm × 20 mm, respectively. The actual thickness of the obtained small specimens was approximately 0.6 mm. After drying and humidification, the specimens had an approximate moisture content of 8 wt% and an average density of 780 kg/m^3. Aniline (≥99.5% purity), phosphoric acid (PA; 85 wt% in H_20, 99.9% trace metal basis), hydrochloric acid (36%–37%), acetone, and ammonium peroxydisulfate (APS) (≥98%) were all purchased from Shanghai InnoChem Science & Technology Co., Ltd. (China).

Methods

Impregnation and polymerization procedure

The bamboo specimens were added to a 2.5 L three-neck flask and weighed down using a metal gauze to prevent the specimens from floating during *in situ* polymerization. The three-neck flask was subjected to vacuum for 30 min to eliminate air from the hollow bamboo structure. Then, 0.2 M of an aqueous aniline solution was prepared, which was the optimum concentration required for polymerization according to a previously published study (Qaiser *et al*. 2012). Next, the obtained aniline solution was mixed with PA in a beaker at 0 °C for 30 min, in which the molar ratio of PA to aniline varied at 0.5, 1, 2, 3, and 4. Next, each of the mixed solutions was rapidly poured into the above three-neck flask containing the bamboo specimens under vacuum; in this process, the specimens were completely submerged so that the reaction solutions could be fully impregnated into the bamboo matrix. Finally, the APS solution was added dropwise into the reaction system of the three-neck flask, and the APS/aniline ratio was 1.25. The reaction was maintained by magnetic stirring under pressure for 6 h; at the same time, the reaction temperature was maintained at 0 to 5 °C throughout the whole process.

After the synthesis of PANI in the bamboo structure, the specimens were removed from the three-neck flask and they were repeatedly washed with a 0.01 M hydrochloric acid and acetone solution to remove the unreacted organics and oligomers. Next, the specimens were repeatedly rinsed with distilled water until a pH of 7 was reached. Finally, the washed specimens were then dried in a vacuum oven at 50 °C for 48 h for further tests.

Weight percent gain (WPG), volume bulking, and equilibrium water uptake

The bamboo specimens were conditioned at 65% RH before impregnation, with the weight and dimensions being measured using a slide caliper at the midpoints of the specimens. The weight and dimensions of the specimens, as well as of the final bamboo products, were then directly measured after being removed from the impregnation solution. This allowed for the calculation of the uptake of the impregnation solution, WPG of the polymer, bulking or volume swelling from polymer uptake, and moisture weight gain of

the bamboo specimens. For a more in-depth description, please refer to a previously published study (Wen *et al.* 2011).

Optical microscopy

Light microscopy was used to observe the appearance of the bamboo/PANI composites; the unmodified bamboo peered veneers were also investigated for comparison. The specimens were sectioned tangentially by cold laser ablation and imaged using an Olympus BX51 optical microscope (Japan).

Scanning electron microscopy (SEM)

The dried tangential sections as well as the cross sections of composites and unmodified bamboo veneers were fixed to a metal stub using a carbon-based putty (LEIT-C-Plast, Ted Pella; USA) and coated with a double layer coating (5 nm) consisting of graphite and gold-palladium using an Agar HR sputter coater (Cressington Ltd., England). The samples were analyzed using a JCM-6000 scanning electron microscope (JEOL Ltd., Japan) operating at an accelerating voltage of 20 kV to capture secondary electron images of the sample surfaces.

Electrical properties

The bamboo/PANI composites were cut into small samples with dimensions of 15 mm × 15 mm (L × W), and then their electrical conductivity was measured at room temperature by a four-point probe method. The multi-height probe was combined with the RM3000 Test Unit (Jandel Engineering Ltd., Germany). The probe was equipped with four tungsten carbide needles having a diameter of 100 µm with a spacing of 1 mm. Sheet resistance (R_s, ohm) was used to calculate the specific resistivity, $\rho = R_s \times A/t$, where A is the cross-sectional area of the sample and t is thickness, and the corresponding conductivity, $\sigma = 1/\rho$ (S/cm).

Fourier transform infrared (FTIR) spectroscopy

The unmodified bamboo peeled veneers and bamboo/PANI were investigated by Fourier transform infrared spectroscopy (Nicolet Magna 560, USA). First, two samples were ground into particles of approximately 60 mesh; then, they were blended with KBr powder and compressed to form a disk. The spectra of each sample were detected in the range from 500 to 4000 cm^{-1} at a resolution of 4 cm^{-1}. As a reference, the PANI powder obtained from the reaction solution after *in situ* polymerization was also investigated by the same procedure.

X-ray diffraction (XRD)

The unmodified bamboo peeled veneers and bamboo/PANI composites were ground into powders of approximately 80 mesh; at the same time, PANI powder was also prepared from the reaction system in the three-neck flask.

The XRD analysis of the three samples was conducted using a diffractometer (D/max 2200, Rigaku, Japan) with Ni-filtered CuKa radiation (k = 1.5406 Å) at 40 kV and 30 mA. In this test, scattered radiation was recorded in the range of $2\theta = 5$ to 50° at a scan rate of 5°/min.

RESULTS AND DISCUSSION

Appearance Characterization

Figure 1 shows the light microscopy images of the appearance of the unmodified bamboo veneer (Fig. 1a) and bamboo/PANI composite (Fig. 1b) in which the PA concentration was 0.6 M.

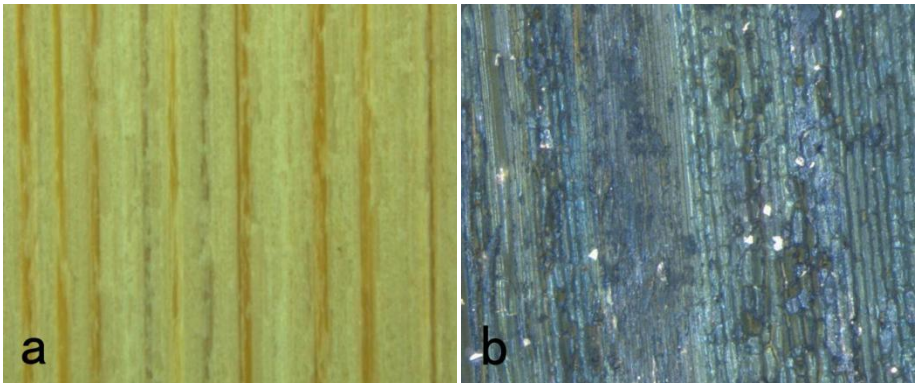

Fig. 1. Light microscopy images of the tangential sections of (a) unmodified bamboo veneer and (b) bamboo/PANI composite

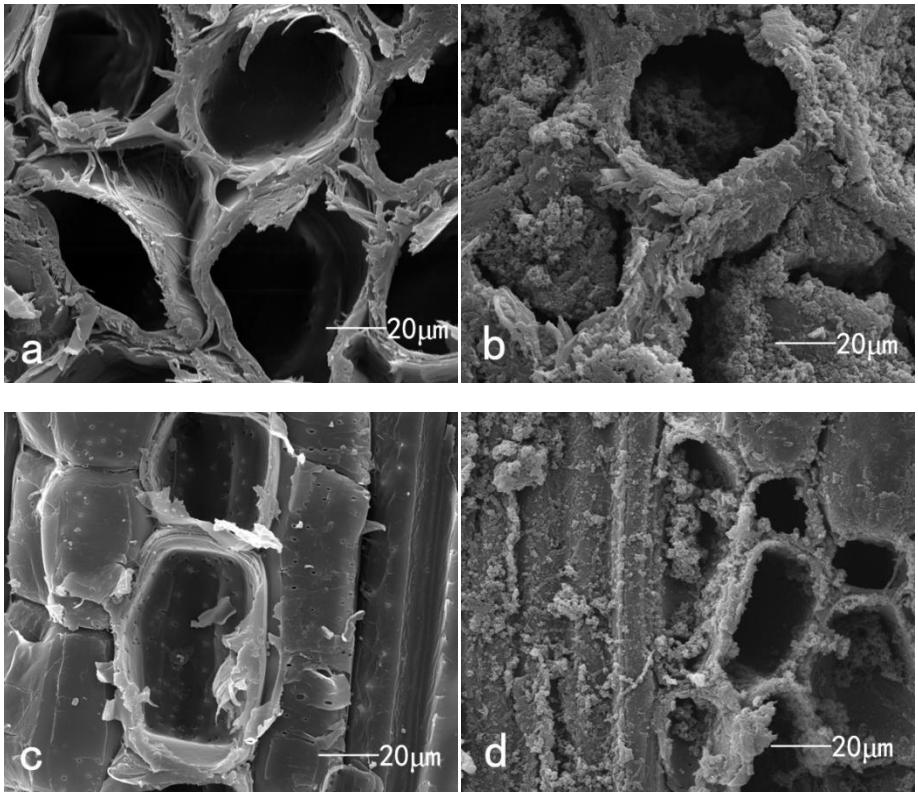

Fig. 2. SEM images of the cross sections of (a) unmodified bamboo veneer and (b) bamboo/PANI composite, and of the tangential sections of (c) unmodified bamboo veneer and (d) bamboo/PANI composite

As shown in Fig. 1b, the bamboo/composite specimen clearly exhibited dark green metallic hues on its surface, implying that PANI particles were homogeneously distributed throughout the bamboo network structure (Trey *et al.* 2012).

To investigate the exact location at which the formation of PANI occurred in the bamboo, SEM was used to image the laser-ablated cross sections of the modified bamboo veneers (Fig. 2a) and bamboo/PANI composites (Fig. 2b); the corresponding images of the tangential sections are shown in Figs. 2c and 2d. Obviously, PANI particles were not observed in the cross section and radial section of the unmodified bamboo specimens, and the porous structure of the bamboo matrix was clearly discerned (Figs. 2a and c). However, for the bamboo/PANI composites, black with green PANI particles were observed in the network, with agglomerates dispersed throughout the bamboo structure (Fig. 1b). At the same time, the PANI particles were clearly observed to be adhered to the bamboo cell wall (Figs. 2b and d).

Weight Percent Gain (WPG), Volume Bulking, and Equilibrium Water Uptake of the Bamboo/PANI Composites

The WPG and volume bulking of bamboo specimens were obtained by a comparison of the weights and dimensions of the dry specimens before and after the *in situ* polymerization of the aniline solution, as shown in Fig. 3. The WPG and volume bulking of the bamboo specimens increased with increasing PA concentration. When the concentration of PA reached 0.6 M, the WPG and volume bulking values were approximately 5.18% and 14.9%, respectively. However, at a PA concentration of 0.8 M, the WPG and volume bulking values decreased. This decrease implies that the aniline solution can polymerize onto the cell walls, resulting in an increase of volume bulking. However, if only PANI was formed in the lumen, no volume swelling would be observed.

By swelling the bamboo/PANI composite specimens in water for 14 days, the water uptake in the bamboo/PANI composites was recorded in comparison with that in the unmodified bamboo specimens, which is shown in Fig. 4.

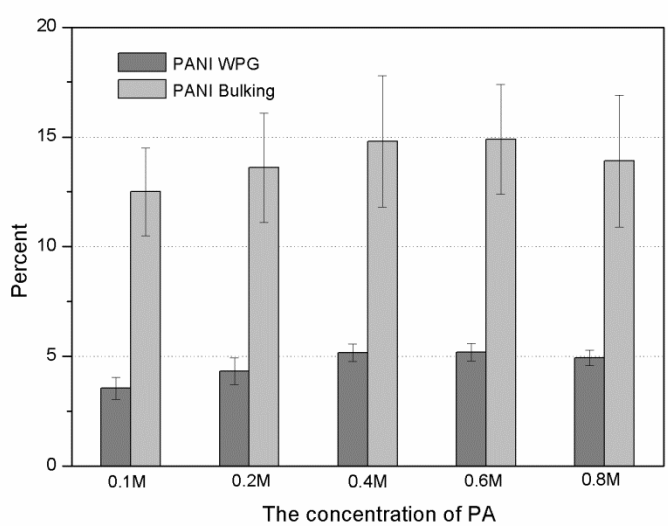

Fig. 3. WPG and volume bulking of the bamboo/PANI composites under different PA concentrations. Data provided as the mean ± standard deviation

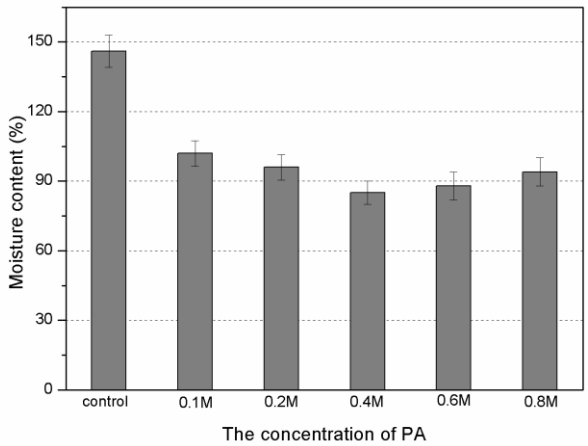

Fig. 4. Equilibrium water uptake of the unmodified bamboo veneer and bamboo/PANI composite specimens under different PA concentrations. Data provided as the mean ± standard deviation

All the bamboo/PANI composites exhibited equilibrium water uptake lower than that of the unmodified bamboo specimens; moreover, the water uptake values of the bamboo/PANI composites gradually decreased with increasing WPG. At a PA concentration of 0.6 M, the bamboo/composite specimen exhibited the lowest equilibrium water uptake value of approximately 82%. This decreased to 43.6% as compared with that of the unmodified bamboo specimen. The water uptake decrease seems likely because hydrophobic PANI filled many of the bamboo cell lumens and cavities, thus preventing the entry of water (Kiemle *et al.* 2003; Venancio *et al.* 2006; Blinova *et al.* 2007a).

Electrical Conductivity

After establishing the location at which PANI formed in the bamboo structure, the next objective was to determine if the combination of PANI and the bamboo substrate could result in a semi-conductive bamboo material, and if so, the minimum concentration of PA needed to achieve it. Unmodified bamboo veneers are insulating materials; hence, they are not shown in Fig. 5.

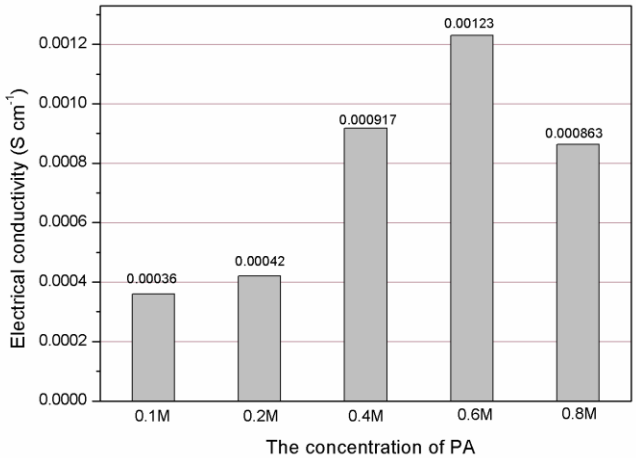

Fig. 5. Electrical conductivity of bamboo/PANI composite under different PA concentrations

The modified bamboo specimens exhibited semi-conductivity comparable with that exhibited by traditional commercial antistatic materials. This was promising, because even with these preliminary results, with a WPG less than 6 wt% (Fig. 3), these conductivity results indicate that aniline enters the cell wall and polymerizes in the wood connective network and not just within the lumen voids. If polymerization had only occurred in the lumen, the polymer would be isolated within closed cells, preventing the connective network needed to result in a conductive material.

On the other hand, the electrical conductivity of the bamboo/PANI composite specimens increased with increasing PA concentration; when the PA concentration increased to 0.6 M, the conductivity reached a maximum of 1.23×10^{-3} S cm^{-1}. Nevertheless, the conductivity of the bamboo/PANI composite decreased once the PA concentration increased beyond this level. These facts indicate that PA concentration significantly affected the electrical conductivity of bamboo/PANI composites. The H^+ concentration increased with increasing PA concentration, which leads to the increase of the electromotive force of aniline toward polymerization. Accordingly, aniline started to oxidize, resulting in the formation of PANI. Meanwhile, the reductive substances of the products started to reduce, and the intermediate substances began to increase, and as a result, the electrical conductivity and yield of PANI increased. With the further increase in the PA concentration, the intermediate state of matter gradually increased, and PA entered the main PANI chains; therefore, the electrical conductivity and yield of PANI continued to increase and finally reached the maximum. However, once the electromotive force of aniline approached the largest electrical potential that aniline has been transformed to the oxidized form of materials, the intermediate substances in PANI started to reduce, thereby leading to the decrease in the electrical conductivity of PANI (Chiang and MacDiarmid 1986; Blinova *et al.* 2006; Blinova *et al*. 2007b).

In summary, the large range of conductivities (1×10^{-4} to 1×10^{-9}) demonstrates that this method is ideal for tuning the conductivity properties.

Fourier Transform Infrared Spectroscopy (FTIR)

Figure 6 shows the FTIR spectra of bamboo, PANI, and bamboo/PANI composite recorded to investigate the morphological characteristics and possible interface bonding between bamboo veneer and PANI in the composites.

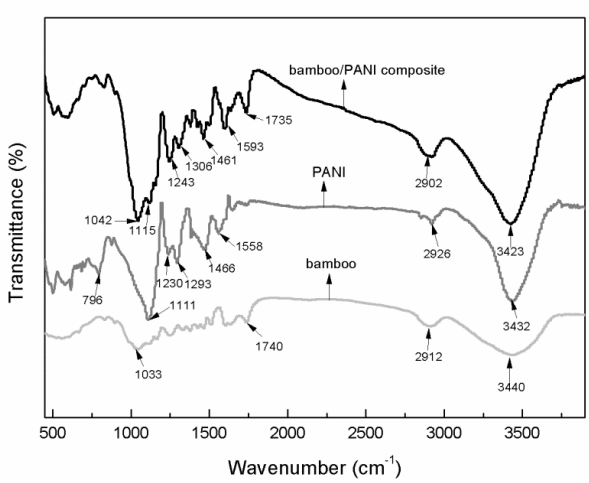

Fig. 6. FTIR spectra of PANI, bamboo veneer, and bamboo/PANI composite

Dominant OH and CH stretching peaks were observed at approximately 3440 and 2912 cm^{-1}, respectively, in the spectra of bamboo veneer (VandenBerg *et al*. 2007). At the same time, a peak was observed at 1740 cm^{-1}, corresponding to the acetyl and uronic ester groups or the ester linkage of the carboxylic group on the ferulic and p-coumaric acids in the hemicelluloses of the bamboo veneer spectra (Socrates 2001). In the FTIR spectrum of PANI, a peak was observed at 796 cm^{-1}, corresponding to the N–H wag of the secondary amine. Furthermore, two additional sharp peaks were observed at 1111 and 1293 cm^{-1}, which were attributed to the aromatic amine. The peaks at 1446 and 1558 cm^{-1} were attributed to the stretching vibrations of N–B–N and N=Q=N structures, respectively (B and Q represent abbreviations for benzenoid and quinoid moieties in the PANI polymers, respectively) (Trchová *et al.* 2005; Rezaei *et al*. 2011; Yu *et al*. 2012).

Although the FTIR spectrum of the bamboo/PANI composite showed the presence of characteristic peaks of both bamboo and PANI, some notable changes were still observed. Most of the characteristic peaks of the bamboo/PANI composite were shifted to lower frequencies than those of pure PANI, which could be ascribed to the cleavage of the hydrogen bonds in PANI particles. On the other hand, the intensity of the OH peak (around 3423 cm^{-1}) in the bamboo/PANI composite significantly increased in comparison with that of bamboo. The fact could be caused by the weakening in the intermolecular hydrogen bonds of bamboo, resulting in the accessibility of more hydroxyl groups in bamboo veneers, which in turn leads to the *in situ* polymerization of PANI on the cell wall.

X-Ray Diffraction (XRD)

Figure 7 shows the XRD curves of the bamboo/PANI composites; the X-ray diffraction curves of bamboo and pure PANI are also shown for comparison purposes.

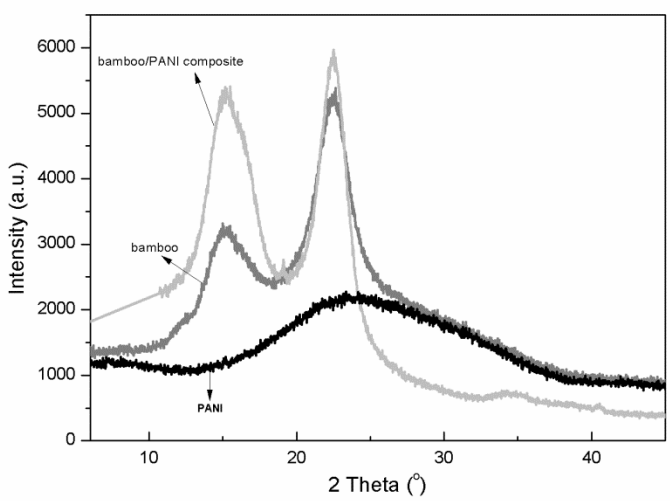

Fig. 7. X-ray diffraction patterns of PANI, bamboo veneer, and bamboo/PANI composite

The X-ray diffraction curve of bamboo showed a classic cellulose I structure, which was evidenced by the peaks located at 15.24° and 22.4° (Pääkkö *et al*. 2007). Similarly, two peaks were observed at 2θ = 21.6° and 24.5°, respectively, in the X-ray diffraction curve of pure PANI (Zhang and Wan 2003; Wang *et al*. 2010). In fact, these peaks were superimposed on a broad scattering centered at *ca.* 2θ = 15 to 25°, which could be ascribed to the periodicity parallel and perpendicular to the polymer chains of PANI, respectively;

these characteristics indicate that PANI is partially crystalline, as previously reported (Ping 1996). Similar to the peaks observed in the XRD curve of bamboo, two peaks were also observed at the same location in the XRD curve of the bamboo/PANI composite, which suggested that the classic cellulose I structure of bamboo is maintained even after the accessibility of PANI. However, the intensity of the peak at 2θ = 15.24° for the bamboo/PANI composites increased sharply, while the intensity of the peak at 2θ = 22° marginally changed. According to the Segal method, 2θ = 15.24° (I_{110}) represents amorphous material, and 2θ = 22.4° (I_{200}) represents both crystalline and amorphous materials (Segal and Meshulam 1979). Therefore, it can be concluded that the degree of crystallinity of bamboo decreases because of the *in situ* polymerization of PANI in the bamboo matrix, in which the intermolecular hydrogen bonds of cellulose are possibly weakened because of the accessibility of more amide groups into the cell wall of bamboo.

CONCLUSIONS

1. In this study, natural bamboo material was modified with intrinsically conductive PANI by *in situ* polymerization. The results indicated that a new semi-conducting material based on bamboo peeled veneer was synthesized; simultaneously, the measurements showed that the equilibrium water uptake of bamboo improves after modification.
2. By changing the concentration of the doping agent (PA), the electrical conductivity of the modified bamboo ranged from 3×10^{-4} to 1×10^{-3} S cm^{-1}, which is suitable for traditional antistatic materials used commercially.
3. Light microscopy images showed that PANI was uniformly dispersed within the cell lumen and cell wall of the bamboo matrix. Furthermore, FTIR spectra and X-ray diffraction analysis indicated that the intermolecular hydrogen bonds of cellulose are possibly weakened because of the accessibility of more amide groups into the cell wall of the bamboo material.

ACKNOWLEDGMENTS

This study was financially supported by the Natural Science Fund in Jiangsu Province (Grant Number BK20140971) and a Project funded by the Science and Technology Development of North Area of Jiangsu (Grant Number BN2014069), as well as the High-level Scientific Research Foundation for the introduction of talent in Nanjing Forestry University (GXL2014068). The authors would like to acknowledge the support of Ms. Qing Cao, Lei Bian, and the teachers of Advanced Analysis & Testing Center of Nanjing Forestry University for SEM and XRD operations.

REFERENCES CITED

Barthet, C., Armes, S. P., Chehimi, M. M., Bilem, C., and Omastova, M. (1998). "Surface characterization of polyaniline-coated polystyrene latexes," *Langmuir* 14(18), 5032-5038. DOI: 10.1021/la980102r

Blinova, N. V., Stejskal, J., Trchová, M., and Prokeš. J. (2006). "Polyaniline prepared in solutions of phosphoric acid: powders, thin films, and colloidal dispersions," *Polymer* 47(1), 42-48. DOI: 10.1016/j.polymer.2005.10.14

Blinova, N. V., Stejskal, J., Trchová, M., Ćirić-Marjanović, G., and Sapurina, I. (2007a). "Polymerization of aniline on polyaniline membrane," *J. Phys. Chem.* B 111(10), 2440-2448. DOI: 10.1021/jp067370f

Blinova, N. V., Stejskal, J., Trchová, M., Prokeš, J., and Omastová, M. (2007b). "Polyaniline and polypyrrole: A comparative study of the preparation," *European Polymer Journal* 43(6), 2331-2341. DOI: 10.1016/j.eurpolymj.2007.03.045

Celzard, A., and Treuseh, O. (2005). "Electrical and elastic properties of new monolithic wood-based carbon materials," *Journal of Materials Science* 40(1), 63-70. DOI: 10.1007/s10853-005-5688-z

Chiang, J. C., and MacDiarmid, A. G. (1986). "Polyaniline protonic acid doping of the emeraldine form to the metallic regime," *Synth. Met.* 13(3), 193-205. DOI: 10.1016/0379-6779(86)90070-6

Dalmolin, C., Biaggio, S. R., Rocha-Filho, R. C., and Bocchi, N. (2009). "Preparation, electrochemical characterization and charge-discharge of reticulated vitreous carbon/polyaniline composite electrodes," *Electrochim. Acta.* 55(1), 227-233. DOI: 10.1016/j.electacta.2009.08.043

Fatyeyeva, K., Pud, A. A., Bardeau, J. F., and Tabellout, M. (2011). "Structure-property relationship in aliphatic polyamide/polyaniline surface layered composites," *Mater. Chem. Phys.* 130(1-2), 760-768. DOI: 10.1016/j.solidstatesciences.2009.03.014

He, W., Nakao, T., Yoshinobu, M., and Zhang, Q. S. (2011). "Treatment of fast-growing poplar with monomers using in-situ polymerization. Part I: Dimensional stability and resistance to biodegradation," *Forest Products J.* 61(2), 113-120.

Hu, W., Chen, S., Yang, Z., Liu, L., and Wang, H. (2011). "Flexible electrically conductive nanocomposite membrane based on bacterial cellulose and polyaniline," *J. Phys. Chem. B* 115(26), 8453-8467. DOI: 10.1021/jp204422v

Jiang, Z. H. (2002). "Bamboo germplasm resource preservation and improvement," in: *Bamboo and Rattan in the World*, Z. H. Jiang (ed.), Liaoning Science and Technology Publishing House, Liaoning, pp. 242-245.

Kawai, S., and Ishihara, S. (1990). "Carbon overlaid Particleboard as an electromagnetic shield and fiber resistive material," *International Timber Engineering Conference*. 10(2), 74-79. DOI: 10.1023/A:1013117131821

Nagasawa, C. (1999). "Electromagnetic shielding particleboard with nickel-plated wood particles," *Journal of Porous Materials* 22(6), 247-254. DOI: 10.1023/A:1013165014982

Oka, H., Fujita, H., and Seki, K. (2000). "Composition and heating efficiency of magnetic wood by induction heating," *IEEE Transactions on Magnetics* 36(5), 3715-3717. DOI: 10.1109/20.914374

Oka, H., Hojo, A., Osada, H., Fujita, H., and Hayakawa, H. (2004). "Manufacturing methods and magnetic characteristics of magnetic wood," *Journal of Magnetism and Magnetic Materials* 272(3), 2332-2334. DOI: 10.1016/j.jmmm.2003.12.1214

Oka, H., and Hayakawa, H. (2002). "Laminated impregnated magnetic wood manufacturing methods and magnetic characteristics from DC to135GHz band," *IEEE Transactions on Magnetics* 38(5), 3327-3328. DOI: 10.1109/20.917621

Pääkkö, M., Ankerfors, M., Kosonen, H., Nykänen, A., Ahola, S., Österberg, M., and Lindstrom, T. (2007). "Enzymatic hydrolysis combined with mechanical shearing and

high-pressure homogenization for nanoscale cellulose fibrils and strong gels," *Biomacromolecules* 8(6), 1934-1941. DOI: 10.1021/bm061215p

Patil, D. S., Shaikh, J. S., Pawar, S. A., Devan, R. S., Ma, Y. R., Moholkar, A. V., John, A., Mahadeva, S. K., and Kim, J. (2010). "The preparation, characterization and actuation behavior of polyaniline and cellulose blended electro-active paper," *Smart Mater. Struct.* 19(4), 0450-0461. DOI: 10.1088/0964-1726/19/4/045011

Ping, Z. (1996). "*In situ* FTIR-attenuated total reflection spectroscopic investigations on the base-acid transitions of polyaniline," *J. Chem. Soc. Farad. Trans* 92(3), 3063-3067. DOI: 10.1039/FT9969203063

Qaiser, A. A., Hyland, M. M., and Patterson, D. A. (2011). "Surface and charge transport characterization of polyaniline-cellulose acetate composite membranes," *J. Phys. Chem. B* 115(7), 1652-1661. DOI: 10.1021/jp109455m

Qaiser, A. A., Hyland, M. M., and Patterson, D. A. (2012). "Effects of various polymerization techniques on PANI deposition at the surface of cellulose ester microporous membranes: XPS and electrical conductivity studies," *Synth. Met.* 162(11-12), 958-967.

Reza, A. (2006). "Application of polyaniline and its composites for adsorption/recovery of chromium from aqueous solutions," *Acta. Chim. Slov.* 53(1), 88-94.

Rezaei, S. J. T., Bide, Y., and Nabid, M. R. (2011). "A new approach for the synthesis of polyaniline microstructures with a unique tetragonal star-like morphology," *Synth. Met.* 161(2), 1414-1419. DOI: 10.1016/j.synthmet.2011.05.011

Rudge, A., Davey, J., Raistrick, I., Gottesfeld, S., and Ferraris, J. P. (1994). "Conducting polymers as active materials in electrochemical capacitors," *J. Power Sources* 47(2), 89-107.

Sathiyanarayanan, S., Jeyaram, R., Muthukrishnan, S., and Venkatachari, G. (2009). "Corrosion protection mechanism of polyaniline blended organic coating on steel," *J. Electrochem. Soc.* 156(4), 127-134. DOI: 10.1149/1.3073874

Segal, A. W., and Meshulam, T. (1979). "Production of superoxide by neutrophils: A reappraisal," *FEBS. Lett.* 100(2), 27-32. DOI: 10.1016/0014-5793(79)81124-2

Shi, X., Zhang, L., Cai, J., Cheng, G., Zhang, H., Li, J., and Wang, X. (2011). "A facile construction of supramolecular complex from polyaniline and cellulose in aqueous system," *Macromolecules* 44(12), 4565-4578. DOI: 10.1021/ma2009904

Shi, Z., Zang, S., Jiang, F., Huang, L., Lu, D., Ma, Y., and Yang, G. (2012). "In-situ nano-assembly of bacterial cellulose-polyaniline composites," *RSC Adv.* 3(2), 1040-1046. DOI: 10.1039/C1RA00719J

Socrates, G. (2001). *Infrared and Raman Characteristic Group Frequencies*, Wiley, New York.

Stejskal, J., Kratochvíl, P., and Jenkins, A. D. (1996). "The formation of polyaniline and the nature of its structures," *Polymer* 37(2), 367-369. DOI: 10.1016/0032-3861(96)81113-X

Trchová, M., Šeděnková, I., and Stejskal, J. (2005). "*In situ* polymerized polyaniline films and FTIR spectroscopic study of aniline polymerization," *Synth. Met.* 154(1), 1-4. DOI: 10.1016/j.synthmet.2005.07.001

Trchová, M., Matějka, P., Brodinová, J., Kalendová, A., Prokeš, J., and Stejskal, J. (2006). "Structural and conductivity changes during the pyrolysis of polyaniline base," *Polym. Degrad. Stab.* 91(2), 114-121. DOI: 10.1016/j.polymdegradstab.2005.04.022

Trey, S., Jafarzadeh, S., and Johansson, M. (2012). "*In situ* polymerization of polyaniline in wood veneers," *ACS Appl. Mater. Interfaces* 4(3), 1760-1769. DOI: 10.1021/am300010s

VandenBerg, O., Schroeter, M., Capadona, J. R., and Weder, C. (2007). "Nanocomposites based on cellulose whiskers and (semi)conducting conjugated polymers," *J. Mater. Chem.* 12(17), 2746-2753. DOI: 10.1039/b700878c

Venancio, E. C., Wang, P. C., and MacDiarmid, A. G. (2006). "The azanes: A class of material incorporating nano/micro self-assembled hollow spheres obtained by aqueous oxidative polymerization of aniline," *Synth. Met.* 156(5-6), 357-369. DOI: 10.1016/j.synthmet.2005.08.035

Wang, X., Wang, X., Wu, Y., Bao, L., and Wang, H. (2010). "Interfacial synthesis of polyaniline nanostructures induced by 5-sulfosalicylic acid," *Mater. Lett.* 64(17), 1865-1867. DOI: 10.1016/j.matlet.2010.06.006

Wolszczak, M., Kroh, J., and Abdel-Hamid, M. M. (1995). "Some aspects of the radiation processing of conducting polymer," *Radiat. Phys. Chem.* 45(1), 71-78. DOI: 10.1016/0969-806X(94)E0025-E

Xiang, X. X., Liu, E. H., Li, L. M., Yang, Y. J., Shen, H. J., Huang, Z. Z., and Tian, Y. Y. (2011). "Activated carbon prepared from polyaniline base by K_2CO_3 activation for application in supercapacitor electrodes," *J. Sol. State Electrochem.* 15(3), 579-585. DOI: 10.1007/s10008-010-1130-9

Yu, H., Wang, C., Zhang, J., Li, H., Liu, S., Ran, Y., and Xia, H., (2012). "Cyclodextrin-assisted synthesis of water-dispersible polyaniline nanofibers by controlling secondary growth," *Mater. Chem. Phys.* 133(1), 459-464. DOI: 10.1016/j.matchemphys.2012.01.065

Article submitted: November 24, 2014; Peer review completed: February 15, 2015; Revised version received and accepted: March 26, 2015; Published: March 31, 2015.
DOI: 10.15376/biores.10.2.2969-2981